Journal of Materials Chemistry A

Accepted Manuscript

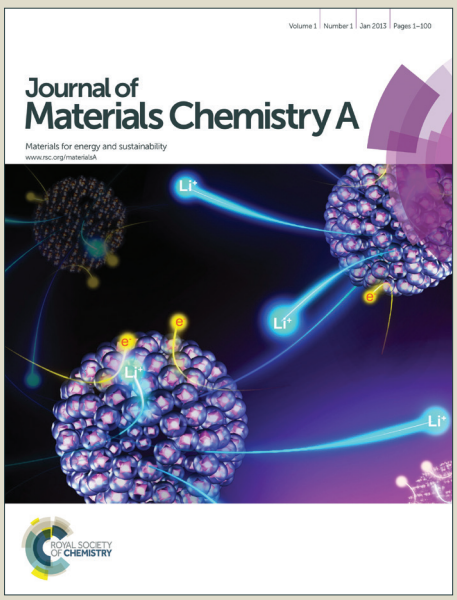

ROYAL SOCIETY OF CHEMISTRY

www.rsc.org/materialsA

Ferromagnetism in Cr-doped passivated AlN nanowires

Mohammed Benali Kanoun,* Souraya Goumri-Said,† and Udo Schwingenschlögl‡

Physical Science and Engineering Division,

King Abdullah University of Science and Technology, Thuwal 23955-6900, Saudi Arabia.

(Dated: March 29, 2014)

Abstract

We apply first principles calculations to predict the effect of Cr doping on the electronic and magnetic properties of passivated AlN nanowires. We compare the energetics of the possible dopant sites and demonstrate for the favorable configuration ferromagnetic ordering. The charge density of the pristine passivated AlN nanowire is used to elucidate the bonding character. Spin density maps demonstrate an induced spin polarization for N atoms next to dopant atoms, though most of the magnetism is carried by the Cr atoms. Cr-doped AlN nanowires turn out to be interesting for spintronic devices.

PACS numbers: 75.50.Cc, 73.61.Ga, 75.30.Hx, 71.15.Mb, 85.75.-d

* mohammed.kanoun@kaust.edu.sa

† Souraya.Goumri-Said@kaust.edu.sa

‡ udo.schwingenschlogl@kaust.edu.sa,+966(0)544700080

Spintronics is currently an active area of research, because spin-based multifunctional devices have several advantages over conventional charge-based devices, including the speed of data processing, nonvolatility, and high integration densities [1, 2]. The interest in such devices has led to growing efforts in developing and designing spintronic materials. Dilute magnetic semiconductors are promising candidates in this regard. While ferromagnetism was discovered in (In,Mn)As [1, 3], for example, it is desirable to have spin polarized charge carriers [4]. Dilute magnetic semiconductors based on III-V compounds have demonstrated a promising combination of unique optoelectronic properties and room-temperature ferromagnetism, with potential industrial applications [5–7]. Various experimental and theoretical efforts have been dedicated to achieving room temperature ferromagnetism while preserving the semiconducting nature of a material. For example, the transition metals Mn, Cr, Fe, Co, V, and Ni have been widely used as magnetic dopants to obtain dilute magnetic semiconductor thin films based on GaN, GaAs, and AlN [8–14], where the origin of the ferromagnetism has been addressed by various authors [15–20].

Recently, the focus has shifted to low-dimensional nanostructures for reducing the device size. Such nanowires, nanotubes, and nanobelts show high thermal stability, chemical resistivity, and excellent mechanical properties. Among the III-nitrides, AlN is interesting for applications in nanoelectronics due to its large bandgap of 6.2 eV [21] and low electron affinity [22]. As a result, AlN-based nanowires [23] have been synthesized recently, including Mn and Mg-doped single-crystal nanowires, which are ferromagnetic with Curie temperatures of up to 300 K [24, 25]. On the theoretical side, Wang and coworkers [18, 26] have contributed to the understanding of the ferromagnetism in Mn-doped GaN nanowires using ab-initio calculations and have suggested that Cr-doped GaN nanowires are more suitable for spintronics. Moreover, Xiang and Wei [27] have argued that surface passivation is a critical factor for sustaining ferromagnetism in Cu-doped GaN nanowires. The ferromagnetism in Mn-doped passivated AlN nanowires has been explored extensively in Refs. [28, 29]. It is therefore important to understand how Cr induces magnetism in low-dimensional passivated systems (where the passivation avoids effects of surface states). To achieve this goal, we have performed a systematic theoretical study of the electronic and magnetic properties of Cr-doped passivated AlN nanowires using first principles calculations.

All calculations are carried out within the framework of spin-polarized density functional theory using the projector augmented wave method as implemented in the Vienna Ab-initio

Simulation Package [30]. Al $3s^2$, $3p^1$, N $2s^2$, $2p^3$, and Cr $3d^5$, $4s^1$ valence states are employed. The exchange-correlation interaction is treated in the generalized gradient approximation using the parametrization of Perdew, Burke and Ernzerhof. To improve the description of electronic correlations in the Cr d shell, an on-site Coulomb interaction of $U = 3.6$ eV and an on-site exchange interaction of $J = 1$ eV are taken into account [31]. The energy cutoff is set to 500 eV. All structures are optimized until the components of the atomic forces have reached values below 0.01 eV/Å. Self-consistency is assumed for an energy difference between two successive iterations of less than 10^{-5} eV. For the Brillouin zone integration, Monkhorst-Pack meshes of $1 \times 1 \times 6$ and $1 \times 1 \times 9$ points are found to be sufficient for the geometry optimizations and electronic structure calculations, respectively.

As starting point, an AlN nanowire with hexagonal cross section enclosed by [1010] facets (infinite along the [0001] direction) is cut from an optimized wurtzite bulk AlN structure with lattice constants of $a = 3.13$ Å and $c = 5.01$ Å, which are in good agreement with the experimental values of $a = 3.11$ Å and $c = 4.98$ Å [32]. To be more specific, the nanowire is generated from a $7 \times 7 \times 2$ wurtzite supercell by removing the Al and N atoms outside a circle of 1 nm diameter, see Fig. 1, and contains 96 atoms (48 Al and 48 N) with about 13 Å vacuum along the $[10\bar{1}0]$ and $[01\bar{1}0]$ directions, thereby ensuring that the nanowires in neighboring supercells do not interact with each other. The infinite extension along the [0001] direction is due to the periodic boundary conditions. H-passivation is used to saturate dangling surface bonds. After optimization of the pristine AlN nanowire, the charge density map on the left hand side of Fig. 2 is generated as the difference between the obtained electron density and the electron densities of the isolated atoms. Clearly, there is a significant amount of charge transferred from the Al to the N atoms, relecting the ionic bonding nature.

In order to evaluate the properties of Cr-doped AlN nanowires, we start by determining the preferable positions of the dopant atoms. To this aim, we replace one Al atom in the 96 atom supercell by Cr, which gives rise to a doping level of 2.1%. The preferable sites are determined by calculating the total energy for Cr replacing (A) the surface three-coordinated Al atom, (B) the surface four-coordinated Al atom in the groove, and (C) the four-coordinated Al atom in the core, see the upper case labels Fig. 1. The total energy for substitution at the A site is found to be 1.07 eV lower than for the B and C sites, indicating that the surface is preferable for substitution. For the A site we obtain an induced magnetic

moment of 3.0 μ_B, which is mainly due to the Cr 3d states (2.5 μ_B), as expected.

To investigate the magnetic interaction between two Cr atoms, six distinct configurations with dopant concentrations of 4.2% (two Al atoms substituted by Cr) are studied, see the lower case labels in Fig. 1. Configurations C-I and C-II correspond to substitution at two nearest and next-nearest neighbor B sites, respectively, whereas in configuration C-III nearest neighbor A and B sites are substituted. Configurations C-IV and C-V are achieved by substituting at two nearest and next-nearest neighbor A sites, respectively. Finally, in configuration C-VI nearest neighbor B and C sites are substituted. To determine the magnetic state, the total energy is calculated for the spin of the two Cr atoms set parallel or antiparallel, representing ferromagnetism (FM) or antiferromagnetism (AFM), where the energy difference $\Delta E = E_{AFM} - E_{FM}$ (per Cr atom) is positive for ferromagnetism. The obtained values and the relative energies with respect to the ground state are collected in Table 1, together with the optimized Cr_1-Cr_2 distances, nearest neighbor Cr-N distances, and magnetic moments. We find always ferromagnetism except for configuration C-II which yields antiferromagnetism.

The relative energies in Table 1 show that configuration C-IV, where the two Cr atoms are bridged by an N atom in the surface layer, is the ground state, indicating that Cr prefers to cluster at the surface. A charge density map for this case is shown on the right hand side of Fig. 2. We note that the Cr_1-N and Cr_2-N bond lengths shorten from 1.89 Å to 1.82 Å and 1.81 Å, respectively. The Cr_1-N-Cr_2 bond angle amounts to 109°. Remarkably, the Cr_1-Cr_2 bond length decreases during the relaxation from 3.07 Å to 2.95 Å. The spin polarization in configuration C-IV is mainly due to the Cr atoms, for which we obtain a local moment of 2.65 μ_B. We note that the adjacent N atoms show small and antiparallelly aligned moments of -0.10 μ_B. Configurations C-III, C-V, and C-VI have higher energies (1.30 eV, 0.05 eV and 2.58 eV, respectively), where the Cr-N bond lengths are close to those of configuration C-IV, but the Cr-Cr bond lengths deviate substantially. Configurations C-I and C-II, in which the two Cr atoms are well separated from each other, are energetically unfavorable, implying that Cr-N-Cr bridges are the determining factor for the stability.

Turning to the electronic structure of the Cr-doped passivated AlN nanowires, we report the density of states (DOS) of the ground state configuration in Fig. 3, which also gives results for the pristine passivated AlN nanowire for comparison. We aim to understand the impact of Cr doping on the electronic states and the Cr-Cr and Cr-N magnetic interactions.

Figure 3(a) exhibits for the pristine passivated AlN nanowire a bandgap of 5.0 eV, close to the value of 4.9 eV calculated in Ref. [33]. The bandgap is larger than in the bulk material (4.1 eV) due to quantum confinement. According to Fig. 3(b), Cr doping introduces in-gap states and spin polarization. This observation is confirmed by the partial DOS curves given in Fig. 3(c), which demonstrate both Cr $3d$ and N $2p$ contributions to the in-gap states. Together with the observed small N magnetic moments we can conclude that the magnetic coupling between Cr atoms is mediated by N bridges. The situation is similar to Cr-doped AlN thin films with ferromagnetic coupling of the Cr atoms in the surface [20]. The spin density obtained for configuration C-IV is displayed in Fig. 4 as isosurface plot. We find a localization at the Cr sites in the surface of the nanowire, whereas the N atoms show much less and the Al atoms virtually no spin polarization, in agreement with Table 1. We can conclude that the additional charge carriers due to Cr doping promote ferromagnetism in passivated AlN nanowires.

We have performed ab-initio calculations to investigate the electronic structure and magnetic properties of Cr-doped passivated AlN nanowires. We find that a single Cr atom prefers to occupy the surface three-coordinated site. Importantly, Cr substitution at the surface results in ferromagnetic coupling between Cr atoms mediated by the N bridge between them. Hybridization between the Cr $3d$ and N $3p$ orbitals leads to small magnetic moments on the adjacent N atoms (antiparallel orientation with respect to the Cr moments). Our results endorses that Cr-doped passivated AlN nanowires are promising for efficiently realizing spin polarized transport and other spin dependent applications.

[1] H. Ohno, Science 1998, 281, 951.

[2] S. A. Wolf, D. D. Awschalom, R. A. Buhrman, J. M. Daughton, S. von Molnar, M. L. Roukes, A. Y. Chtchelkanova, and D. M. Treger, Science 2001, 294, 1488.

[3] H. Munekat, H. Ohno, S. von Molnar, A. Segmüller, L. L. Chang, and L. Esaki, Phys. Rev. Lett. 1989, 63, 1849.

[4] H. Ohno, Nat. Mater. 9, 952 (2010).

[5] M. A. Mayerm, P. R. Stone, N. Miller, H. M. Smith, O. D. Dubon, E. E. Haller, K. M. Yu, W. Walukiewicz, X. Liu, and J. K. Furdyna, Phys. Rev. B 2010, 81, 045205.

[6] A. H. MacDonald, P. Schiffer, and N. Samarth, Nat. Mater. 2005, 4, 195.

[7] Q. Liu, C. X. Liu, C. Xu, X. L.Qi and S. C. Zhang, Phys. Rev. Lett. 2009, 102, 156603.

[8] T. Dietl, H. Ohno, F. Matsukura, J. Cibert, and D. Ferrand, Science 2000, 287, 1019.

[9] S. Y. Wu, H. X. Liu, L. Gu, R. K. Singh, L. Budd, M. Schilfgaarde, M. R. MaCartney, D. J. Smith, and N. Newman, Appl. Phys. Lett. 2003, 82, 3047.

[10] D. Kumar, J. Antifakos, M. G. Blamire and Z. H. Barber, Appl. Phys. Lett. 2004, 84, 5004.

[11] A. Y. Polyakov, N. B. Smirnov, A. V. Govorkov, R. M. Frazier, J. Y. Liefer, G. T. Thaler, C. R. Abernathy, S. J. Pearton, and J. M. Zavada, Appl. Phys. Lett. 2004, 85, 4067.

[12] R.M. Frazier, G. T. Thaler, J. Y. Leifer, J. K. Hite, B. P. Gila, C. R. Abernathy, and S. J. Pearton, Appl. Phys. Lett. 2005, 85, 052101.

[13] J. Zhang, X. Z. Li, B. Xu and D. J. Sellmyer, Appl. Phys. Lett. 2005, 86, 212504.

[14] A. Titov, X. Biquard, D. Halley, S. Kuroda, E. Bellet-Amalric, H. Mariette, J. Cibert, A. E. Merad, M. B. Kanoun, E. Kulatov, and Y. A. Uspenskii, Phys. Rev. B 2005, 72, 115209.

[15] M. van Schilfgaarde and O. N. Mryasov, Phys. Rev. B 2001, 63, 233205.

[16] K. Sato and H. Katayama-Yoshida, Semicond. Sci. Technol. 2002, 17, 367.

[17] M. B. Kanoun, S. Goumri-Said, A. E. Merad, and J. Cibert, J. Phys. D: Appl. Phys. 2005, 38, 1853.

[18] Q. Wang, Q. Sun, P. Jena, and Y. Kawazoe, Nano Lett. 2005, 5, 1587.

[19] T. Jungwirth, J. Sinova, J. Masek, J. Kucera and A. H. MacDonald, Rev. Mod. Phys. 2006, 78, 809.

[20] Q. Wang, A. K. Kandalam, Q. Sun, and P. Jena, Phys. Rev. B 2006, 73, 115411.

[21] J. Li, K. B. Nam, M. L. Nakarmi, J. Y. Lin, H. X. Jiang, P. Carrier and S.-H. Wei, Appl. Phys. Lett. 2003, 83, 5163.

[22] V. N. Tondare, C. Balasubramanian, S. V. Shende, D. S. Joag, V. P. Godbole, S. V. Bhoraskar and M. Bhadbhade, Appl. Phys. Lett. 2002, 80, 4813.

[23] K. T. Kenry, K. Yong, andS. F. Yu, J. Mater. Sci. 2012, 47, 5341.

[24] Y. Yang, Q. Zhao, X. Z. Zhang, Z. G. Liu, C. X. Zou, B. Shen, and D. P. Yu, Appl. Phys. Lett. 2007, 90, 092118.

[25] Y. Xu, B. Yao, D. Liu, W. Lei, P. Zhu, Q. Cui, and G. Zoua, Cryst. Eng. Comm. 2013, 15, 3271.

[26] Q. Wang, Q. Sun, and P. Jena, Phys. Rev. Lett. 2005, 95, 167202.

[27] H. J. Xiang and S. H. Wei, Nano Lett. 2008, 8, 1825.

[28] Y. Zhang, H. Shi, R. Li and P. Zhang, Phys. Lett. A 2011, 375, 1686

[29] Z. K. Tang, L. L. Wang, L. M. Tang, X. F. Li,W. Z. Xiao, L. Xu and L. H. Zhao, Phys. Status Solidi B, 2012, 249, 185.

[30] G. Kresse and J. Furthmüller, Comput. Mater. Sci. 1996, 6, 15.

[31] P. Gopal and N. A. Spaldin, Phys. Rev. B 2006, 74, 094418.

[32] J. H. Edgar, Properties of Group-III Nitrides, EMIS Data Reviews Series (IEE, London, 1994).

[33] M. L. Colussi, R. J. Baierle, and R. H. Miwa, J. Appl. Phys. 2011, 110, 033709.

[34] H. Akai, Phys. Rev. Lett. 1998, 81, 3002.

TABLE I. Energy difference between antiferromagnetism and ferromagnetism, relative energy with respect to the ground state (configuration C-IV), optimized Cr1-Cr2 and Cr-N distances, and magnetic moments of the Cr and N atoms. Energies are given in eV, distances in Å, and moments in μ_B.

Configuration	ΔE	$\Delta\varepsilon$	$d_{\text{Cr1-Cr2}}$	$d_{\text{Cr1-N}}$	μ_{Cr1}	μ_{Cr2}	μ_{N}	Coupling
C-I (a,b)	0.19	2.62	4.33	1.82	2.58	2.53	−0.04	FM
C-II (a,c)	−1.28	4.10	4.86	1.83	2.53	2.51	−0.03	AFM
C-III (a,d)	0.08	1.30	3.05	1.83	2.49	2.50	−0.08	FM
C-IV (d,e)	1.64	0.00	2.95	1.81	2.67	2.60	−0.10	FM
C-V (d,f)	0.06	0.05	3.15	1.83	2.76	2.76	−0.04	FM
C-VI (a,g)	0.34	2.58	3.08	1.84	2.71	2.52	−0.04	FM

Figures captions

Fig. 1: Passivated AlN nanowire. The positions of Cr substitution are marked by letters. The gray, blue, and white spheres represent Al, N, and H atoms, respectively.

Fig. 2: Charge density distribution in the surface plane of the (left) undoped and (right) Cr-doped passivated AlN nanowire.

Fig. 3: (a) Total density of states of the undoped AlN nanowire. Spin-polarized (b) total and (c) partial Cr $3d$, Al $3p$ and N $2p$ density of states of the Cr-doped passivated AlN nanowire. The vertical solid line denotes the Fermi level.

Fig. 4: Spin density distribution in the Cr-doped passivated AlN nanowire.

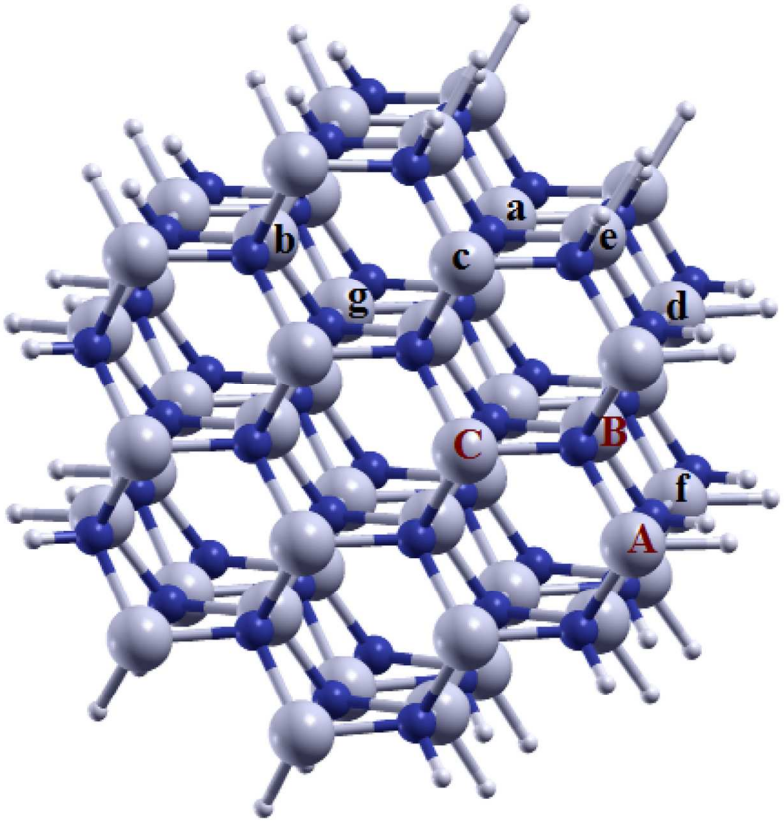

135x125mm (300 x 300 DPI)

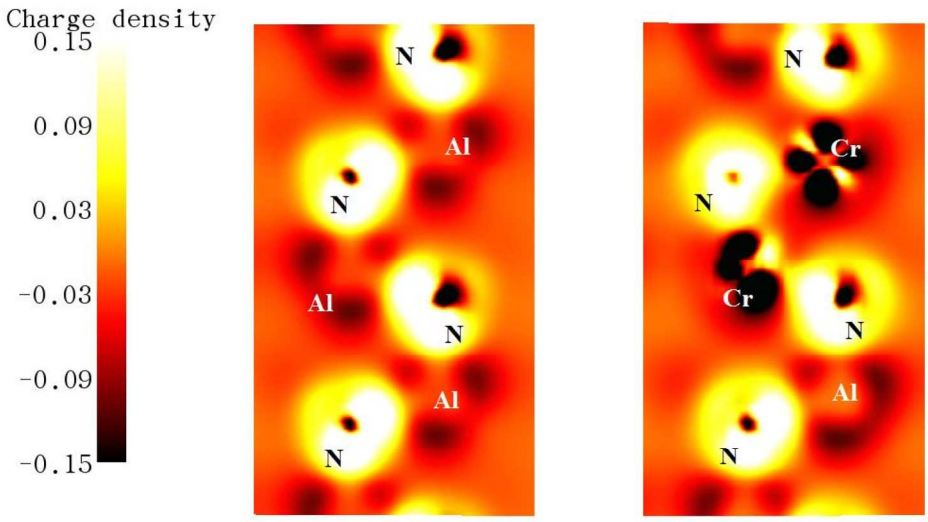

159x90mm (300 x 300 DPI)

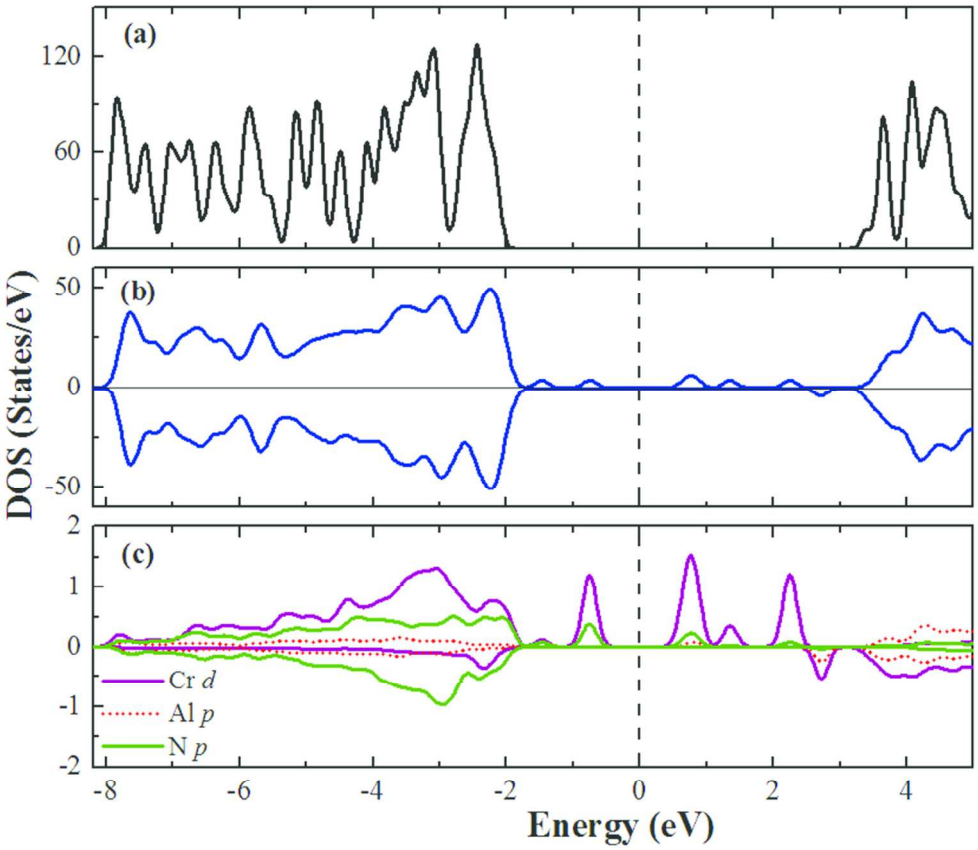

Figure 3

93x91mm (300 x 300 DPI)

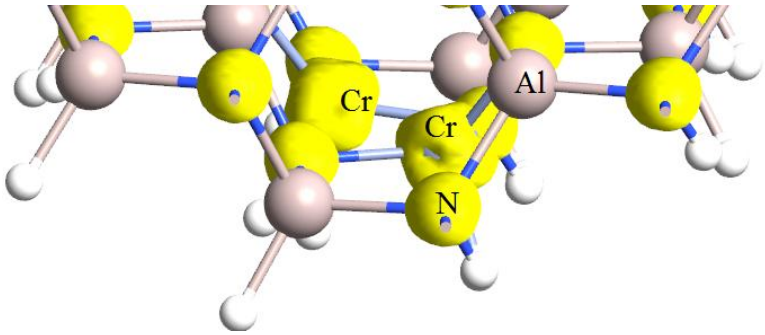

Figure 4